CYLINDER DECOMPOSITIONS ON GEOMETRIC ARMADILLO TAILS

DAMI LEE AND JOSH SOUTHERLAND

ABSTRACT. We study a particular type of finite area, infinite-type translation surfaces, and find explicit examples of types of cylinder decompositions on these surfaces which do not manifest on finite-type translation surfaces.

1. INTRODUCTION AND DEFINITIONS

A translation surface is a (countable) collection of polygons in the plane where all edges are paired with an edge of equal length by translation such that inward pointing normal vectors for each edge point in opposite directions after identification. Finite-type translation surfaces are collections of finitely many polygons with only finitely many edges, whereas infinite-type translation surfaces allow for constructions containing countably many polygons allowing infinitely many edges. See, for example, [4].

In this article, we define a particular infinite-type translation surface to study, which we call an *armadillo tail surface*, or *armadillo tail*. We place a square, which we denote by $\square_1$, in the first quadrant so that the lower left vertex lies at the origin and all edges are parallel to the axes. For $k \geq 1$, glue the left side of $\square_{k+1}$ to the right side of $\square_k$ so that the bottom edge of all squares lie on the x-axis. We denote the side length of $\square_k$ by l_k, and assume that (l_k) is a strictly decreasing sequence. We then identify horizontal (vertical, resp.) edges via vertical (horizontal, resp.) translation. Bowman [2] and Degli Esposti–Del Magno–Lenci [3] have also built infinite-type translation surfaces in a similar fashion but allowed rectangles instead of squares; the surface in the former article is known as a "stack of boxes" and the one in the latter, "Italian billiards."

The following are examples of finite-area armadillo tail surfaces.

Example 1.1. (1) The armadillo tail surface where $l_k = r^{k-1}$, for $r \in (0,1)$, which we call a *geometric armadillo* with parameter r. Its area is $\frac{1}{1-r^2}$.

(2) The *harmonic armadillo tail* where $l_k = \frac{1}{k}$. While the surface is not bounded in the horizontal direction, its area is $\zeta(2) = \frac{\pi^2}{6}$, finite.

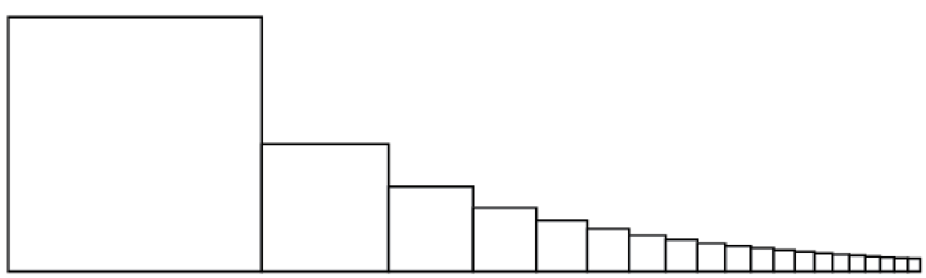

FIGURE 1. The harmonic armadillo tail surface

We attain a finite translation surface we call the *truncated armadillo tail* which is $\bigcup_{k=1}^{n} \square_k$ where we make the same identifications as above, except that we identify the right edge of $\square_n$ with the bottom segment of the left edge of $\square_1$. We denote the truncated armadillo tail by X_n.

Without loss of generality, we assume that $l_1 = 1$. With horizontal (vertical, resp.) edges being identified via vertical (horizontal, resp.) translation, the resulting translation surface is an infinite genus surface (infinite connected sum of square tori) with one (wild) singularity. For background on wild singularities, see [2], [4], [8]. The wild singularity appears infinitely many times in the polygonal representation of the surface: each vertex of the infinite-sided polygon is the same point on the surface.

Armadillo tails are concrete, toy examples that we use for prodding at both the geometric and dynamical properties of finite area, infinite-type translation surfaces with one wild singularity (and no other singularities). In what follows, our focus is on a purely geometric construction: a cylinder decomposition on this surface. Finding cylinder decompositions on a surface is challenging, even on finite translation surfaces. Here, we are able to leverage the structure of the surface to inductively construct cylinders.

We begin with definitions, and an example, before stating the main result. A *cylinder* is a closed subspace of the surface whose interior is foliated by homotopic closed straight-line trajectories, and whose boundary consists of saddle connections, line segments whose endpoints coincide with a singular point. A closed geodesic in a cylinder is called a *waist curve*. The *circumference* of a cylinder is the length of a closed straight-line trajectory, and the *width* of a cylinder is the distance between the bounding saddle connections. A *cylinder decomposition* is the closure of a union of possibly infinitely many cylinders whose waist curves are in the same direction and which covers the surface. Further, we require that each cylinder in the cylinder decomposition only intersect another cylinder at most along a saddle connection. The closure of the union of cylinders may contain a line segment that is not in any cylinder which we call a *spine*. If a spine is made of a single saddle connection, we call it a *rigid spine*. If a spine is comprised of multiple (possibly infinitely many) saddle connections, we call it a *flexible spine*. If a cylinder decomposition has no spine, we say it is a *complete cylinder decomposition*.

As an example, consider the cylinder decomposition $\mathcal{C}$ of an armadillo tail in the rather obvious horizontal direction, given our choice of polygonal representation of the surface. See Figure 2.

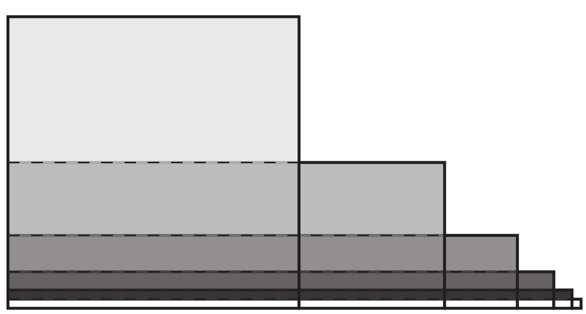

FIGURE 2. A cylinder decomposition of a geometric armadillo tail in the horizontal direction

Observe that as we move from top to bottom, each cylinder in the cylinder decomposition becomes longer and thinner, eventually limiting to a concatenation of infinitely many cylinders at the base of the polygonal representation. This may appear to be a flexible spine, but each of these saddle connections is a boundary component of a cylinder, namely "top" of a cylinder, since the bottom saddle connections are the same as the the saddle connections appearing at the top of each square. Indeed, this is a complete cylinder decomposition.

There is another cylinder decomposition intimately related to the above cylinder decomposition, what we call the *orthogonal cylinder decomposition*, $\mathcal{C}^{\perp}$. In the original cylinder decomposition shown in Figure 2, label the cylinders numerically from top to bottom, cyl_k. Then, $\text{cyl}_1^{\perp}$, the first cylinder in $\mathcal{C}^{\perp}$ has width equal to the circumference of cyl_1 in $\mathcal{C}$. The circumference of $\text{cyl}_1^{\perp}$ is equal to the sum of all of the widths of the cylinders in the original cylinder decomposition. Similarly, the $\text{cyl}_2^{\perp}$ has width equal to the height of cyl_2 less the height of cyl_1. The circumference of $\text{cyl}_2^{\perp}$ is the sum of all of the widths of the cylinders in $\mathcal{C}$ less the width of cyl_1. Each subsequent cylinder is defined in the same manner. See Figure 3.

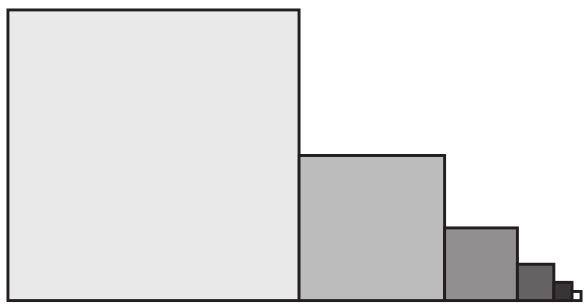

FIGURE 3. A cylinder decomposition of an armadillo tail in the vertical direction

Remark 1.2. Observe that the modulus of each cylinder in the orthogonal cylinder decomposition is 1. This implies that there exists an affine diffeomorphism of the surface ϕ such that $D\phi = \begin{bmatrix} 1 & 0 \\ 1 & 1 \end{bmatrix}$, where $D\phi$ is an element in the Veech group. See Appendix D in [5] for additional information. Observe that $D\phi$ is a parabolic element in $SL_2(\mathbb{R})$, where the eigendirection of $D\phi$ corresponds to the direction of the cylinder decomposition. We will refer to an affine diffeomorphism whose derivative is a parabolic element as a *parabolic affine diffeomorphism*. A parabolic affine diffeomorphism is an example of a reducible element in the mapping class group of the underlying surface.

1.1. **Main results.** There is another less obvious cylinder decomposition on the surface which does not appear in the orbit of this horizontal cylinder decomposition (orbit of the group of affine automorphisms of the surface). In the same way that the above cylinder decomposition is comprised of an infinite number of cylinders limiting to a spine, this cylinder decomposition will also. However, the distinction is that this one limits to a rigid spine, not a flexible spine.

Theorem 1.3. There exists a cylinder decomposition limiting to a rigid spine on any geometric armadillo tail of parameter $\frac{1}{q}$, $q \in \mathbb{N} \setminus \{1\}$. Moreover, there is no parabolic affine diffeomorphism of the surface that fixes this cylinder decomposition.

The proof of the theorem is constructive. In Section 2, we identify a core curve in a special direction, which turns out to be a rigid spine of a cylinder decomposition. This curve wraps around every torus in the surface. Then we construct a cylinder which turns out to be the widest cylinder in the cylinder decomposition. In Section 3, we inductively construct a collection of saddle connections which turn out to frame all of the cylinders in our cylinder decomposition. In Section 4, we construct the cylinder decomposition by defining a (discontinuous) map which pushes a cylinder to a subset of the next widest cylinder in the decomposition. We call the subset of a cylinder a "partial cylinder." See Section 4 for a definition. We "fill in" the missing segments of the cylinder using a circle rotation argument. Indeed, the endpoints of the partial cylinder correspond to periodic points of a circle rotation. In Section 5, we compute the modulus and area of each cylinder in the cylinder decomposition.

It seems feasible to extend our methods to the case of $r = \frac{p}{q}$, provided one can find enough cylinders to start the induction process. Moreover, the induction process may involve fixed points of a finite-type interval exchange transformation (IET) in lieu of a circle rotation. See [10] for a description of IETs.

In Section 6, we show that there cannot be a parabolic element that stabilizes the cylinder decomposition that we construct. Moreover, we note that the orthogonal cylinder decomposition to this cylinder decomposition *does not exist*.

1.2. **Related work.** Bowman studies the "geometric limit" of finite translation surfaces converging to an infinite-type translation surface [1]. Along these lines, we can think of a geometric armadillo tail as the limit of finite-type translation surfaces. Indeed, consider the truncated surface X_n. The cylinder decomposition in the special direction persists for all surfaces in this sequence. Moreover, for all finite surfaces in the sequence, there is a parabolic element that preserves both this cylinder decomposition and another that preserves the orthogonal cylinder decomposition. However, in the limit, the cylinders converge to a cylinder decomposition, but the parabolic affine diffeomorphism does not converge to any sensible affine map on the surface.

For particular directions on an armadillo tail, one can use Treviño's work, Theorem 3 in [9], to see if one can conclude that the linear flow in that direction is ergodic. However, there does not appear to be a (Veech) dichotomy in which each direction is either periodic or ergodic: the Veech group appears to be $\mathbb{Z}$ and not a lattice. It is an interesting question as to what ergodic measures are supported on an armadillo tail (geometric or otherwise). A generalization of a Veech dichotomy of this flavor was done for infinite staircase surfaces by Hooper, Hubert, and Weiss [6].

Lastly, there is an open question regarding whether or not there exists a finite area, infinite-type translation surface with a Veech group that is a lattice in $SL_2(\mathbb{R})$ (see [4]). One might think that a particular geometric armadillo tail is a candidate, but it seems as though the Veech group may be $\mathbb{Z}$. A proof that the Veech group is $\mathbb{Z}$ would be interesting.

1.3. **Acknowledgements.** The authors would like to thank David Aulicino, Matt Bainbridge, and Pat Hooper for helpful conversations.

2. THE SPINE (OR A PARTICULAR DIRECTION ON GEOMETRIC ARMADILLO TAILS)

The following is a key theorem in which we identify a closed saddle connection which turns out to be a (limiting) rigid spine of a cylinder decomposition on a certain family of armadillo tails. Every armadillo tail is an infinite connected sum of tori; this particular saddle connection wraps around each torus. Note that the following theorem is very general and requires no assumption on the parameter r. By $\frac{1}{2-r}$-direction, we mean the direction with slope $\frac{1}{2-r}$ relative to our polygonal representation.

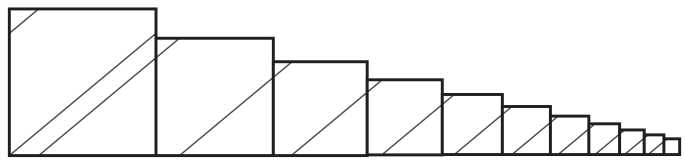

FIGURE 4. A geometric armadillo tail ($r = 4/5$) with a trajectory of slope $\frac{5}{6} = \frac{1}{2-r}$

Theorem 2.1. On geometric armadillo tails for any $r \in (0, 1)$, there exists a closed saddle connection in the $\frac{1}{2-r}$-direction that intersects every torus.

Proof. We refer to the top (horizontal) edge of a square by the *roof* and the right (vertical) edge of a square that is identified to a segment on the y-axis by the *portal.*

We start from the origin, the lower left vertex of $\square_1$. Since $r < \frac{1}{2-r} < 1$, the straight line of slope $\frac{1}{2-r}$ through the origin hits the portal of $\square_1$ at point $(1, \frac{1}{2-r})$. By identification with the y-axis (the left edge of $\square_1$), the trajectory continues and hits the roof of $\square_1$ at $(1-r, 1)$. By identification with the bottom edge of $\square_1$, the trajectory continues from $(1-r, 0)$ and hits the roof of $\square_2$ at $(1 + r(1-r), r)$. The trajectory partitions both roofs with a fixed ratio. Hence, due to similarity in consecutive squares, it continues to hit every roof partitioning them with the same ratio. Needless to say, the trajectory "wraps around every torus" without hitting any vertex. $\square$

Via renormalization (under the action of $\begin{pmatrix} 1 & 0 \\ -1 & 1 \end{pmatrix}$, see Remark 1.2), one can consider the trajectory with slope $\frac{1}{2-r} - 1 = \frac{r-1}{2-r}$ direction. Starting from the upper left vertex at $(0, 1)$, the trajectory hits the portal on $\square_1$ at $\left(1, \frac{1}{2-r}\right)$. By identification, continuing from $\left(0, \frac{1}{2-r}\right)$, the trajectory does not hit any roof or portal and tends to $\left(\frac{1}{1-r}, 0\right)$, hence producing a saddle connection. In fact, given our polygonal representation, any trajectory starting from $(0, 0)$ with slope $\frac{1}{2-r} + \mathbf{n}$, for any $\mathbf{n} \in \mathbb{N}$, (or $(0, 1)$ with slope $\frac{1}{2-r} - \mathbf{n}$, for $\mathbf{n} \in \mathbb{N}$) yields a saddle connection that goes through every torus. We will see that this saddle connection is the rigid spine of a cylinder decomposition.

Moreover, the saddle connection of Theorem 2.1 has an interesting topological feature.

Proposition 2.2. The saddle connection of Theorem 2.1 is a non-separating simple closed curve.

Proof. If we color the surface on one side of the saddle connection, we will color the entire surface. $\square$

In the following theorem, we show that for a specific family of geometric armadillo tails, i.e., when $r = \frac{1}{q}$ for $q \in \mathbb{N} \setminus \{1\}$, there exists not only a saddle connection but a cylinder in the $\frac{1}{2-r}$-direction. (Figure 5) We call this cylinder cyl_1, and the existence of this cylinder will be part of the base case for the induction that follows.

Theorem 2.3. Given any geometric armadillo tail with parameter $r = \frac{1}{q}$, there exists a cylinder in the $\frac{1}{2-r}$-direction which lies entirely in $\square_1 \cup \square_2$.

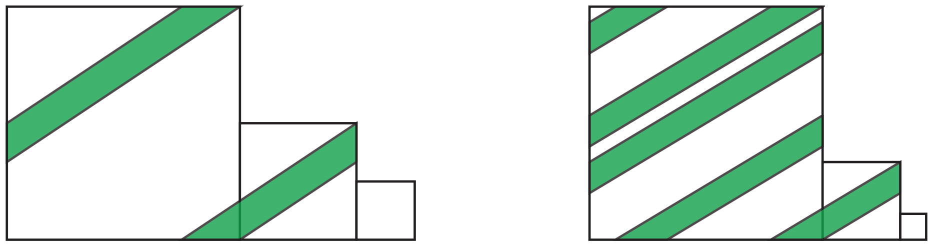

FIGURE 5. The cylinder cyl_1 on a geometric armadillo tail with parameter $1/2$ (left) and $1/3$ (right)

There are three parts to this proof. First, we show that there is a saddle connection (in the $\frac{1}{2-r}$-direction) that lies entirely in X_2. Secondly, we will show that there is another saddle connection in X_2 parallel to the first one. In the third step, we will show that there is no saddle connection between the two saddle connections, and consequently that the interstitial space is foliated by closed geodesics, hence yielding a cylinder.

Proof. Note, for $q = \mathbb{N} \setminus \{1\}$, the slope of the trajectory is $\frac{1}{2-r} = \frac{q}{2q-1}$.

Step 1. We show that the trajectory from $(1,0)$ with slope $\frac{q}{2q-1}$ stays entirely in X_2.

Start from $(1,0)$ we hit the portal of $\square_2$ at $\left(1+\frac{1}{q}, \frac{1}{2q-1}\right)$, hence the first point at which the trajectory hits the vertical axis is at $\left(0, \frac{1}{2q-1}\right)$. We continue and hit $\left(1, \frac{1+q}{2q-1}\right)$, and since $\frac{1}{q} < \frac{1+q}{2q-1} < 1$, the trajectory goes through the portal and is identified to $\left(0, \frac{1+q}{2q-1}\right)$. Note that if we keep hitting the portal, the nth time the trajectory hits the vertical axis is at $\left(0, \frac{1}{2q-1} + \frac{(n-1)q}{2q-1} - \lfloor \frac{1}{2q-1} + \frac{(n-1)q}{2q-1} \rfloor \right)$. In fact, since $\frac{1}{2q-1} < \frac{1}{q} < \frac{2}{2q-1}$, we will always hit the portal unless the numerator of $\frac{1}{2q-1} + \frac{(n-1)q}{2q-1} - \lfloor \frac{1}{2q-1} + \frac{(n-1)q}{2q-1} \rfloor$ is 1. Pick $n = 2q-2$, then the trajectory hits the singularity at $(1,1)$. In other words, the trajectory goes through $\square_2$ exactly once at the beginning and stays in $\square_1$ until it hits a singularity.

Furthermore, this is the first time the trajectory hits the singularity. This follows from the fact that $\gcd(q, 2q-1) = 1$. The trajectory hits the y-axis at points $\left\{(0,y) : y \in \left\{ \frac{(n-1)q+1}{2q-1} - \lfloor \frac{(n-1)q+1}{2q-1} \rfloor \right\}\right\}$. Note that the numerator of the y-coordinates in this set is

$$\{1, 1+q, 1+2q, \ldots, 1+(2q-3)q \equiv 0 \mod (2q-1)\}.$$

Note that if we had continued to add $\frac{q}{2q-1}$, we would have hit $\frac{1+(2q-2)q}{2q-1} \equiv \frac{q}{2q-1}$ and $\frac{1+(2q-1)q}{2q-1} \equiv \frac{1}{2q-1}$, which brings us back to the beginning of the sequence. In other words, the trajectory wraps around $\square_1$ exactly $2q-3$ times hitting the y-axis at $\left\{\left(0, \frac{i}{2q-1}\right)\right\}_{i=1,\neq q}^{2q-2}$.

Alternatively, notice that once the trajectory enters square one, we can encode the hitting points on the portal (which are identified to the left side of square 1) via a circle rotation that arises as a section of the linear flow with slope $\frac{q}{2q-1}$. We use this perspective in Step 2 and 3 below.

Step 2. The saddle connection that we constructed above will serve as the "bottom" boundary saddle connection of cyl_1. Next, we will construct a saddle connection which will end up being the "top" boundary saddle connection. To do this, we will take the bottom saddle connections and show that if we shift the saddle connection vertically (in the polygonal representation) by $\frac{q-1}{q(2q-1)}$, that we find another saddle connection. A consequence of step 3, which follows, is that $\frac{q-1}{q(2q-1)}$ is the *skew-width* of this cylinder, the vertical distance (with respect to the polygonal representation) between the two saddle connections. The skew-width is formally defined in Section 3.

Take the set of points where the bottom saddle connection hits the y-axis and add $\frac{q-1}{q(2q-1)}$:

$$\left\{\frac{i}{2q-1}\right\}_{i=1,\neq q}^{2q-2} + \frac{q-1}{q(2q-1)} = \left\{\frac{(i+1)q-1}{q(2q-1)}\right\}_{i=1,\neq q}^{2q-2},$$

where a set + number denotes adding the number to each element of the set. We split this set into three cases: (1) $i = 1, \ldots, q-2$, (2) $i = q-1$, and (3) $i = q+1, \ldots, 2q-2$.

Define $T : [0,1]/\sim \to [0,1]/\sim$ be a circle rotation where $T(x) = x + \frac{q}{2q-1}$. Note that the circle rotation is a section of the linear flow on $\square_1$, provided we never enter $\square_2$. We can guarantee that the linear flow does not enter $\square_2$ provided the iterates of the circle rotation are greater than or equal to $\frac{1}{q}$. Observe that every point in the set $\left\{\frac{(i+1)q-1}{q(2q-1)}\right\}_{i=1,\neq q}^{2q-2}$ is greater than or equal to $\frac{1}{q}$. Moreover, the image of these points under T is always greater than $\frac{1}{q}$, except for the image of the point corresponding to case (2): $i = q-1$. We will address this when it arises.

First, observe that T maps points corresponding to case (1) to a points corresponding to case (3). Indeed, take points in (1), ($i = 1, \ldots, q-2$), and apply T. We have

$$T\left(\frac{(i+1)q-1}{q(2q-1)}\right) = \frac{(i+1+q)q-1}{q(2q-1)} \in \left\{\frac{(j+1)q-1}{q(2q-1)}\right\}_{j=q+1}^{2q-1}.$$

Next, observe that the points in case (3) map to points in case (1), with one exception, in which case the image of point corresponds to the point in case (2). Take points in case (3), ($i = q+1, \ldots, 2q-2$) and apply T. For all points except $i = 2q-2$ we have

$$T\left(\frac{(i+1)q-1}{q(2q-1)}\right) = \frac{(i+1+q)q-1}{q(2q-1)} \equiv \frac{(i-q+2)q-1}{q(2q-1)} \in \left\{\frac{(j+1)q-1}{q(2q-1)}\right\}_{j=1}^{q-2}.$$

If $i = 2q-2$, then we have $T\left(\frac{(2q-1)q-1}{q(2q-1)}\right) = \frac{q^2-1}{q(2q-1)} \in \left\{\frac{(i+1)q-1}{q(2q-1)}\right\}_{i=q-1}$, which corresponds to the point in case (2).

Lastly, consider the point in case (2), where $i = q-1$. We have

$$T\left(\frac{q^2-1}{q(2q-1)}\right) = \frac{2q^2-1}{q(2q-1)} \equiv \frac{q-1}{q(2q-1)} < \frac{1}{q}.$$

Since the trajectory hits the right side of $\square_1$ below the portal, we continue into $\square_2$ and hit $\left(1+\frac{1}{q}, \frac{1}{q}\right)$, the singularity at the upper right vertex of $\square_2$.

Now, observe that if we begin with $i = 1$, the sequence of iterates of T will include every point in case (1) and case (3), and then hit the point in case (2). In other words, the suspension of the linear flow is a closed saddle connection that passes through $\left(0, \frac{1}{q}\right)$ that lies entirely in $\square_1$ and $\square_2$.

Step 3. Lastly, we show that between these two saddle connections there is no other saddle connection in with slope $\frac{q}{2q-1}$. In other words, there are no saddle connections that hit the vertical axis between $\left(0, \frac{1}{2q-1}\right)$ and $\left(0, \frac{1}{q}\right)$.

Define the intervals along the y-axis with y-coordinates in $\left(\frac{i}{2q-1}, \frac{i}{2q-1} + \frac{q-1}{q(2q-1)}\right)$, for $i \in \{1, 2, \cdots, 2q-2\} \setminus \{q\}$. The lower bound in each interval coincides with an intersection of the (bottom) saddle connection constructed in step 1 with the y-axis. Similarly, the upper bound coincides with an intersection of the (top) saddle connection constructed in step 2 with the y-axis.

First, observe that the intervals do not contain a singularity. The only appearances of the wild singularity along the y-axis for $y > \frac{1}{2q-1}$ occur for $y = \frac{1}{q}$ and $y = 1$, neither of which land inside any of the intervals.

Now, fix any $0 < \varepsilon < \frac{q-1}{q(2q-1)}$ and consider the collection of points $(0, y_i)$ for $y_i = \frac{i}{2q-1} + \varepsilon$, for $i \in \{1, 2, \cdots, 2q-2\} \setminus \{q\}$. (There is one point in each of the intervals.) By applying the map T to the point in the interval corresponding to $i = 1$, we see that the the image is the point in the collection corresponding to the interval $i = q+1$. The argument is the same as the one given in step (2). We continue applying the map T until we reach the last interval in the set, $(0, y_{q-1})$. Here the image of the circle rotation contains the singular point infinitely many times, but this is because the circle rotation no longer applies. Indeed, $T(y_{q-1}) < \frac{1}{q}$ which means that the suspended flow is actually entering $\square_2$. (This is identical to the situation described in case (2) in step 2.) If we flow in the linear direction from $(0, y_{q-1})$, we hit the portal in $\square_2$ at $(1 + \frac{1}{q}, y_1)$, which means that the linear flow starting at $(0, y_1)$ is a closed geodesic.

Moreover, since the choice of ε allows for any point in the interval, the suspension of these intervals consists of closed geodesics.

In conclusion, on a geometric armadillo tail with parameter $r = \frac{1}{q}$, there exists a cylinder that lies entirely in $\square_1$ and $\square_2$. We call this cylinder cyl_1. $\square$

Remark 2.4. The assumption that $r = \frac{1}{q}$ cannot be removed. For example, if $r = 2/3$, the saddle connection starting from $(1, 0)$ is not contained in $\square_1$ and $\square_2$, but also passes through $\square_3$.

3. Framing (or finding the bottom saddle connection of each cylinder by induction)

This section provides the construction of saddle connections that later become a part of the bottom saddle connection of each cylinder. In the following, Lemma 3.2 shows this for $k = 2$, and Theorem 3.3 generalizes this for all k.

Notation 3.1. In what follows, we will construct sets of saddle connections $\mathrm{bsc}_{k,q}$. In Section 4, these sets will be realized as the **b**ottom boundary **s**addle **c**onnection of the k^{th} widest cylinder in the cylinder decomposition on the geometric armadillo with parameter $\frac{1}{q}$. To reduce the notational complexity, and since most of the following statements fix q, we will write bsc_k in lieu of $\mathrm{bsc}_{k,q}$.

In the following lemma, for every $q \in \mathbb{N} \setminus \{1\}$, we construct a single saddle connection that lies in the set bsc_2. We use the linear flow with slope $\frac{q}{2q-1}$, but the reader may also interpret the work as identifying fixed points of an IET arising from a section of the linear flow.

Lemma 3.2. Given any geometric armadillo tail with parameter $r = \frac{1}{q}$, $q \in \mathbb{N} \setminus \{1\}$, we can construct a saddle connection called bsc_2'.

Proof. We use the following notations:

- $\xrightarrow{x}$ indicates the linear flow where the horizontal displacement is x,
- $\xrightarrow{\text{portal}(\#)}$ indicates that the flow hit a portal of $\square_\#$, i.e., the x-coordinate is $1 + \cdots + \frac{1}{q^{\#-1}}$ and the y-coordinate lies between $\frac{1}{q^\#}$ and $\frac{1}{q^{\#-1}}$, hence it is mapped to the corresponding point on the y-axis.
- $\xrightarrow{\text{roof}(\#)}$ indicates that the flow passed the roof of $\square_\#$, i.e., the point is not on the polygonal representation of the surface, hence the y-coordinate is to be adjusted.

We show that a linear flow in the $\frac{q}{2q-1}$-direction from $\left(1+\frac{1}{q},0\right)$ contains the top saddle connection of cyl_1.

$$\left(1+\frac{1}{q},0\right) \xrightarrow{\frac{1}{q^2}} \left(1+\frac{1}{q}+\frac{1}{q^2},\frac{1}{q(2q-1)}\right) \xrightarrow{\text{portal}(3)} \left(0,\frac{1}{q(2q-1)}\right)$$
$$\xrightarrow{1} \left(1,\frac{1+q^2}{q(2q-1)}\right) \xrightarrow{\text{portal}(1)} \left(0,\frac{1+q^2}{q(2q-1)}\right) \xrightarrow{\text{roof}(1)} \left(1,\frac{1+q}{q(2q-1)}\right).$$

All operations above apply to all $q \in \mathbb{N} \setminus \{1\}$. Observe that $\frac{1+q}{q(2q-1)} = \frac{1}{q}$ if $q = 2$, and $\frac{1+q}{q(2q-1)} < \frac{1}{q}$ if $q > 2$.

If $q = 2$, the linear flow in the $\frac{q}{2q-1}$-direction from $\left(1+\frac{1}{q},0\right)$ to $\left(1,\frac{1+q}{q(2q-1)}\right)$ is a saddle connection, bsc_2'.

If $q > 2$, we have $\frac{1+q}{q(2q-1)} < \frac{1}{q}$. Hence we do not yet have a saddle connection. Continuing from the last expression we have,

$$\left(1,\frac{1+q}{q(2q-1)}\right) \xrightarrow{\frac{1}{q}} \left(1+\frac{1}{q},\frac{1+2q}{q(2q-1)}\right) \xrightarrow{\text{roof}(2)} \left(1+\frac{1}{q},\frac{2}{q(2q-1)}\right)$$
$$\xrightarrow{\text{portal}} \left(0,\frac{2}{q(2q-1)}\right) \xrightarrow{1} \left(1,\frac{2+q^2}{q(2q-1)}\right) \xrightarrow{\text{portal}} \left(0,\frac{2+q^2}{q(2q-1)}\right)$$
$$\xrightarrow{1} \left(1,\frac{2+2q^2}{q(2q-1)}\right) \xrightarrow{\text{roof}(1)} \left(1,\frac{2+q}{q(2q-1)}\right).$$

Note that $\frac{2+q}{q(2q-1)} = \frac{1}{q}$ if $q = 3$, and $\frac{2+q}{q(2q-1)} < \frac{1}{q}$ if $q > 3$. Hence we have a saddle connection bsc_3'.

Induction hypothesis $\frac{n+q}{q(2q-1)} = \frac{1}{q}$ if $q = n+1$.

Inductive step We show that $\frac{n+1+q}{q(2q-1)} = \frac{1}{q}$ if $q = n+2$.

Assume that the linear flow has not yielded a saddle connection yet, i.e., $n > q-1$. Then,

$$\left(1,\frac{n+q}{q(2q-1)}\right) \xrightarrow{1/q} \left(1+\frac{1}{q},\frac{n+2q}{q(2q-1)}\right) \xrightarrow{\text{roof}(2)} \left(1+\frac{1}{q},\frac{n+1}{q(2q-1)}\right)$$
$$\xrightarrow{\text{portal}} \left(0,\frac{n+1}{q(2q-1)}\right) \xrightarrow{1} \left(1,\frac{n+1+q^2}{q(2q-1)}\right) \xrightarrow{\text{portal}} \left(0,\frac{n+1+q^2}{q(2q-1)}\right)$$
$$\xrightarrow{1} \left(1,\frac{n+1+2q^2}{q(2q-1)}\right) \xrightarrow{\text{roof}(1)} \left(1,\frac{n+1+q}{q(2q-1)}\right)$$

Since $\frac{n+1+q}{q(2q-1)} = \frac{1}{q}$ for $n+1 = q-1$, this concludes our proof that bsc_2' exists for all $q \in \mathbb{N} \setminus \{1\}$. □

In the following Lemma, for every $q \in \mathbb{N} \setminus \{1\}$, we construct a single saddle connection that lies in the set bsc_k for an integer $k > 2$. The previous Lemma serves as the base case for an induction proof that show the existence of this saddle connection

Theorem 3.3. Given any geometric armadillo tail with parameter $r = \frac{1}{q}$, $q \in \mathbb{N} \setminus \{1\}$, there exists a saddle connection that we call bsc_k'.

Proof. We use the same notations we did in the previous lemma.

$$\left(1+\cdots+\frac{1}{q^{k-1}},0\right)\xrightarrow{1/q^k}\left(1+\cdots+\frac{1}{q^k},\frac{1}{q^{k-1}(2q-1)}\right)$$
$$\xrightarrow{\text{portal}}\left(0,\frac{1}{q^{k-1}(2q-1)}\right)\xrightarrow{1}\left(1,\frac{1+q^k}{q^{k-1}(2q-1)}\right)$$
$$\xrightarrow{1}\left(1,\frac{1+2q^k}{q^{k-1}(2q-1)}\right)$$
$$\xrightarrow{\text{roof}(1)}\left(1,\frac{1+q^{k-1}}{q^{k-1}(2q-1)}\right).$$

The last point above is a singularity if $q=2$ and $k=2$, however, we assume k is large enough and continue.

$$\cdots\xrightarrow{1/q}\left(1+\frac{1}{q},\frac{1+2q^{k-1}}{q^{k-1}(2q-1)}\right)\xrightarrow{\text{roof}(2)}\left(1+\frac{1}{q},\frac{1+q^{k-2}}{q^{k-1}(2q-1)}\right).$$

Again, the last expression is a singularity if $q=2$ and $k=3$.

Induction hypothesis For l sufficiently less than k, assume

$$\left(1+\cdots+\frac{1}{q^l},\frac{1+q^{k-l-1}}{q^{k-1}(2q-1)}\right)$$

is a singularity if $q=2$.

Inductive step We show that

$$\left(1+\cdots+\frac{1}{q^{l+1}},\frac{1+q^{k-l-2}}{q^{k-1}(2q-1)}\right)$$

is a singularity if $q=2$.

For $q>2$, we then have

$$\xrightarrow{1/q^{l+1}}\left(1+\cdots+\frac{1}{q^{l+1}},\frac{1+2q^{k-l-1}}{q^{k-1}(2q-1)}\right)$$
$$\xrightarrow{\text{roof}(l+2)}\left(1+\cdots+\frac{1}{q^{l+1}},\frac{1+q^{k-l-2}}{q^{k-1}(2q-1)}\right),$$

and the last expression is a singularity if $q=2$, and this proves our hypothesis.

Let $l=k-3$, then the last expression becomes $\left(1+\cdots+\frac{1}{q^{k-2}},\frac{1+q}{q^{k-1}(2q-1)}\right)$, which is a singularity for $q=2$. For $q>2$, we have

$$\left(1+\cdots+\tfrac{1}{q^{k-2}},\tfrac{1+q}{q^{k-1}(2q-1)}\right)\xrightarrow{1/q^{k-1}}\left(1+\cdots+\tfrac{1}{q^{k-1}},\tfrac{1+2q}{q^{k-1}(2q-1)}\right)$$
$$\xrightarrow{\text{roof}(k)}\left(1+\cdots+\tfrac{1}{q^{k-1}},\tfrac{2}{q^{k-1}(2q-1)}\right)\xrightarrow{\text{portal}}\left(0,\tfrac{2}{q^{k-1}(2q-1)}\right)$$
$$\xrightarrow{1}\left(1,\tfrac{2}{q^{k-1}(2q-1)}\right).$$

We claim that the rest follows from the induction technique used in the Lemma 3.2. □

Define bsc_1 to be the saddle connection constructed in Step 1 of Theorem 2.3. Then define bsc_2 to be the concatenation of two saddle connections, one being the one constructed in Step 2 of Theorem 2.3, the other being bsc_2'. Observe that we can write $\text{bsc}_2 = \text{bsc}_1 + \frac{q-1}{q(2q-1)} \cup \{\text{bsc}_2'\}$, where $\cup$ means concatenate, and addition means shifting the saddle connections in the set vertically by $\frac{q-1}{q(2q-1)}$. To do this carefully, we need to remove the singular point(s) from the saddle connections, then vertically shift, and then take the closure. (A vertical shift is not well-defined at a singular point.)

We will use this observation to inductively construct the sets bsc_k which will be realized in Section 4 as the bottom saddle connections of the k^{th} widest cylinder. We begin by constructing the set bsc_3. This will be our base case.

Lemma 3.4. Define $\text{bsc}_3 = \text{bsc}_2 + \frac{q-1}{q^2(2q-1)} \cup \{\text{bsc}_3'\}$. Then bsc_3 is a concatenation of 2 saddle connections.

Proof. Clearly, bsc_2' is one of the two saddle connections. We show that $\text{bsc}_2 + \frac{q-1}{q^2(2q-1)}$ yields a single saddle connection.

Idea: start at $(0, 1 - \frac{1}{q} - \frac{1}{q^2}) = (0, X + \frac{q-1}{q^2(2q-1)})$. Circle rotate until you hit under $\frac{1}{q}$. The sc should then flow out to hit a singularity at the top right of square 3. □

Lemma 3.5. Define $\text{bsc}_{k+1} = \text{bsc}_k + \frac{q-1}{q^k(2q-1)} \cup \{\text{bsc}_{k+1}'\}$. Then bsc_{k+1} is a concatenation of 2 saddle connections.

Proof. We prove this by induction, where Lemma 3.4. Assume that bsc_k is a a single saddle connection. It suffices to show that $\text{bsc}_k + \frac{q-1}{q^k(2q-1)}$ is a single saddle connection. □

Theorem 3.6. The trajectory here means two saddle conections trajectory starting from $\left(1 + \frac{1}{q} + \cdots + \frac{1}{q^{k-1}}, 0\right)$ in the $\frac{q}{2q-1}$-direction, i.e., bsc_k hits $\{([0, y) : 0 < y < 1\}$ at

$$\begin{aligned}
&\left\{\left\{\frac{1}{2q-1}, \dots, \widehat{\frac{q}{2q-1}}, \dots, \frac{2q-2}{2q-1}\right\} + \sum_{i=1}^{k-1} \frac{q-1}{q^i(2q-1)}\right\} \\
\cup\ &\left\{\left\{\frac{i}{q(2q-1)}, \frac{i+q^2}{q(2q-1)}\right\}_{i=1}^{q-1} + \sum_{i=2}^{k-1} \frac{q-1}{q^i(2q-1)}\right\} \\
&\vdots \\
\cup\ &\left\{\left\{\frac{i}{q^{j-1}(2q-1)}, \frac{i+q^j}{q^{j-1}(2q-1)}\right\}_{i=1}^{q-1} + \sum_{i=j}^{k-1} \frac{q-1}{q^i(2q-1)}\right\} \\
&\vdots \\
\cup\ &\left\{\frac{i}{q^{k-1}(2q-1)}, \frac{i+q^k}{q^{k-1}(2q-1)}\right\}_{i=1}^{q-1}
\end{aligned}$$

where "set + number" indicates that the number is added to every element in the set.

Proof. This set is constructed inductively using the □

4. Finding successive cylinders in the $\frac{1}{2-r}$-direction

Definition 4.1. Given cyl_k, we define the *skew-width of cyl_k* as the vertical distance (vertical in relation to the polygonal representation) between the two boundary saddle connections of cyl_k through the cylinder.

The definition of skew-width above needs to find its home.

In this section, we use induction to construct the bottom saddle connection of the kth cylinder and hence the cylinder themselves in the $\frac{1}{2-r}$-direction.

We define a map f_r to construct new cylinders from existing cylinders.

Definition 4.2. The map $\tilde{f}_r : \mathbb{R}^2 \to \mathbb{R}^2$, where

$$\tilde{f}_r : \begin{pmatrix} x \\ y \end{pmatrix} \mapsto \begin{pmatrix} rx+1 \\ ry \end{pmatrix}.$$

Observe that $\tilde{f}_r$ is an injective map.

The map does not descend from $\mathbb{R}^2$ to a well-defined map on the quotient of the polygonal representation of an armadillo tail. The issue is that the map does not respect the vertical gluings (by horizontal translations). For instance, the leftmost edge of $\square_1$ is mapped to the leftmost edge of $\square_2$, but the leftmost edge of $\square_2$ is glued to the right edge of $\square_2$. However, the map does descend to a partial quotient, where we only identify the top and bottom edges, since $\tilde{f}_r$ respects the identifications along the tops and bottoms of the squares. That is the content of the following lemma, whose proof is elementary.

Lemma 4.3. Let P_r be the polygonal representation of an armadillo tail X with parameter r such that the polygonal representation is embedded in $\mathbb{R}^2$ and the edge identifications forgotten. Let X^{tb} be a quotient of P_r by identifying the top and bottom edges only. Let $\square_k^{tb}$ denote the kth-square in X^{tb}. Then $\tilde{f}_r$ descends to a map f_r on X^{tb}. The image of $\square_k^{tb}$ under f_r is $\square_{k+1}^{tb}$.

Let $q : P_r \to X^{tb}$ be the quotient map identifying the top and bottom edges of the polygon. Let cyl_k be a cylinder, and lift cyl_k to X^{tb}. Call this lift cyl_k^{tb}. Let L and R denote the unidentified left and right edges of the polygon. Inductively define cyl_{k+1} as the closure of $q \circ f_r(\mathrm{cyl}_k^{tb} \setminus (L \cup R))$ with respect to the linear flow in the $\frac{1}{2-r}$-direction. Observe that cyl_{k+1} does not depend on the chosen lift of cyl_k.

Given a geometric armadillo tail with parameter $r = 1/q$, first we show that cyl_k lies entirely on $X_{k+1} = \bigcup_{i=1}^{k+1} \square_i$. Then $q \circ f_r(\mathrm{cyl}_k)$ is a subset of a cylinder that lies in $X_{k+1}^{tb} \setminus \square_1$. We will show that there is a circle rotation on $\{0\} \times [0,1]$ that fills in $q \circ f_r(\mathrm{cyl}_k)$ at the points of discontinuity.

We define where the circle rotation is defined, and prove that waist curves of cylinders are periodic points under the circle rotation.

We define the *generation zone* as the preimage of cyl_1 in $X \setminus \square_1$ under f_r:

$$\begin{aligned} \text{generation zone} &:= f_r^{-1}(\mathrm{Int}(\mathrm{cyl}_1 \cap \square_2)) \\ &= \left\{ (x,y) : \frac{1}{2-r}x < y < \frac{1}{2-r}x + \frac{1-r}{2-r}, 0 \le x \le 1 \right\}. \end{aligned}$$

Given the set of points where cyl_k intersects $\{0\} \times [0,1]$ and $\{1\} \times [0,1]$, we remove the points that lie in the generation zone. Define sets S_1 (and S_2, resp.) on $\{0\} \times [0,1]$ (and $\{1\} \times [0,1]$, resp.) as the image of the remaining points under f_r. That is,

$$S_1 = \mathrm{proj}_y \circ f_r \left(\gamma \cap \left\{ (0,y) : 0 < y < \frac{1}{2-r} \right\} \right)$$

and

$$S_2 = \left\{ f_r \left(\gamma \cap \left\{ (0,y) : \frac{1-r}{2-r} < y < 1 \right\} \right) \right\}$$

where $\mathrm{proj}_y(x,y) = (0,y)$ is the projection onto the y-axis.

Recall the circle rotation $T(x) = x + \frac{q}{2q-1}$. Note that $q \circ f_r(\mathrm{cyl}_k) \subset X^{tb} \setminus \square_1$ is a subset of a cylinder. Since the circle rotation is a section of the linear flow, we "fill in" $q \circ f_r(\mathrm{cyl}_k)$ at the points of discontinuity to construct cyl_{k+1}. Figure 6 illustrates the setting.

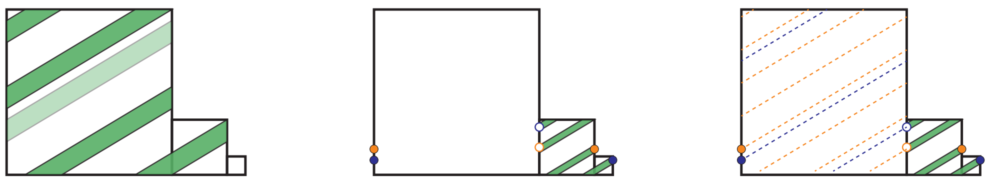

FIGURE 6. $\mathrm{cyl}_1 \setminus$ generation zone(left), $f_r\,(\mathrm{cyl}_1 \setminus \text{generation zone})$ (center), connecting S_1 and S_2 via the circle rotation T (right). The dotted lines represent bsc_2 in $\square_1$.

We illustrate the simplest case ($k = 1$) before we prove the general case for all k. Since we can explicitly write the points at which bsc_1 intersects the y-axis (Theorem 2.3), we consider bsc_1 instead of the waist curves of cyl_1. These points are

$$\left\{ \frac{1}{2q-1}, \ldots, \widehat{\frac{q}{2q-1}}, \ldots, \frac{2q-2}{2q-1} \right\},$$

hence we have

$$S_1 = \left\{ (0,y) : y = \frac{1}{q(2q-1)}, \ldots, \frac{q-1}{q(2q-1)} \right\}, \quad S_2 = \left\{ (1,y) : y = \frac{q-1}{q(2q-1)}, \ldots, \frac{2q-2}{q(2q-1)} \right\}.$$

Take $i = 1, \ldots, q-2$, then

$$\frac{i}{q(2q-1)} \xrightarrow{T} \frac{i+q^2}{q(2q-1)} \xrightarrow{T} \frac{i+2q^2}{q(2q-1)} \equiv \frac{i}{q(2q-1)},$$

where $\frac{1}{q} < \frac{i+q^2}{q(2q-1)} < 1$ for $i \in \{1, \ldots, q-2\}$. We note that $\left\{ \left(0, \frac{i+q^2}{q(2q-1)}\right) \right\}_{i=1}^{q-2}$ are $q-2$ additional points where we hit the y-axis.

When $i = q-1$,

$$\frac{q-1}{q(2q-1)} \xrightarrow{T} \frac{q-1+q^2}{q(2q-1)} \xrightarrow{T} \frac{q-1+2q^2}{q(2q-1)} \equiv \frac{2q-1}{q(2q-1)}.$$

First note that $\left(1, \frac{2q-1}{q(2q-1)}\right)$ is a singularity. Take γ to be a waist curve slightly above this to avoid the singularity and carry on by iterating T. Moreover, note that $T^{2q-1}\left(\frac{q-1}{q(2q-1)}\right) = \frac{q-1+(2q-1)q^2}{q(2q-1)} \equiv \frac{q-1}{q(2q-1)}$. We will show below that for any $m < 2q-1$, the mth iterate hits the portal of $\square_1$, i.e., $\frac{1}{q} < T^m(\frac{q-1}{q(2q-1)}) = \frac{q-1+mq^2}{q(2q-1)} < 1$. This adds an additional $q-2$ points where we hit the y-axis.

Lemma 4.4. Given a geometric armadillo tail with parameter $1/q$, and an infinite cylinder decomposition in the $\frac{q}{2q-1}$-direction, the skew-width of cyl_k is $\frac{q-1}{q^k(2q-1)}$, and the width of cyl_k is $\frac{q-1}{q^k\sqrt{q^2+(2q-1)^2}}$.

Theorem 4.5. The circle rotation $T : [0,1]/\sim \to [0,1]/\sim$ where $T(x) = x + \frac{q}{2q-1}$ maps S_1 to S_2 defined above.

Proof. Theorem 3.6 tells us exactly where bsc_k intersects $\{[0,y] : 0 < y < 1\}$. Recall that S_1 consists of points on $\{0\} \times [0,1]$ whose y-coordinates are

$$\frac{1}{q}\left(\bigcup_{j=1}^{k-1}\left\{\left\{\frac{i}{q^{j-1}(2q-1)}\right\}_{i=1}^{q-1}+\sum_{i=j}^{k-1}\frac{q-1}{q^i(2q-1)}\right\}\cup\left\{\frac{i}{q^{k-1}(2q-1)}\right\}_{i=1}^{q-1}\right)$$

and S_2 consists of points on $\{1\} \times [0,1]$ whose y-coordinates are

$$\begin{aligned}&\frac{1}{q}\left\{\left\{\frac{q-1}{2q-1},\frac{q+1}{2q-1},\dots,\frac{2q-2}{2q-1}\right\}+\sum_{i=1}^{k-1}\frac{q-1}{q^i(2q-1)}\right\}\\ \cup\ &\bigcup_{j=2}^{k-1}\frac{1}{q}\left\{\left\{\frac{i+q^j}{q^{j-1}(2q-1)}\right\}_{i=1}^{q-1}+\sum_{i=j}^{k-1}\frac{q-1}{q^i(2q-1)}\right\}\\ \cup\ &\frac{1}{q}\left\{\frac{i+q^k}{q^{k-1}(2q-1)}\right\}_{i=1}^{q-1}.\end{aligned}$$

These can be simplified to

$$S_1=\left\{(0,y): y\in\bigcup_{j=1}^{k-1}\left\{\frac{(i+1)q^{k-j}-1}{q^k(2q-1)}\right\}_{i=1}^{q-1}\cup\left\{\frac{i}{q^k(2q-1)}\right\}_{i=1}^{q-1}\right\}$$

and

$$S_2=\left\{(1,y): y\in\left\{\frac{(1+i)q^{k-1}+q^k-1}{q^k(2q-1)}\right\}_{i=-1,i\neq 0}^{q-2}\cup\bigcup_{j=2}^{k-1}\left\{\frac{(1+i)q^{k-j}+q^k-1}{q^k(2q-1)}\right\}_{i=1}^{q-1}\cup\left\{\frac{i+q^k}{q^{k-1}(2q-1)}\right\}_{i=1}^{q-1}\right\}.$$

We will show that under some iterate of T, S_1 maps onto S_2. We will break this down into three cases. In each case, we show that a point in S_1 maps to a point in S_2 under T^2 (or T^{2q-1}) but any fewer iterate of T maps it to the complement of S_2 on $\{1\}\times[0,1]$, i.e., $\left\{(1,y) : \frac{q}{2q-1} < y < 1\right\}$.

Case 1. First we have $T\left(\frac{i}{q^k(2q-1)}\right) = \frac{i+q^k}{q^k(2q-1)}$ for any $i \in \{1,\dots,q-1\}$.

Case 2-1. Consider the cases where $j = 2,\dots,k-1$, and $i = 1,\dots,q-1$. Then

$$T^2\left(\frac{(i+1)q^{k-j}-1}{q^k(2q-1)}\right)=\frac{(i+1)q^{k-j}-1+2q^{k+1}}{q^k(2q-1)}\equiv\frac{(i+1)q^{k-j}-1+q^k}{q^k(2q-1)}.$$

We show that $T\left(\frac{(i+1)q^{k-j}-1}{q^k(2q-1)}\right)$ does not hit any point in S_2, i.e.,

$$\frac{1}{q}<\frac{(i+1)q^{k-j}-1+q^{k+1}}{q^k(2q-1)}<1.$$

The left inequality holds since it is equivalent to the inequalities below:

$$\begin{aligned}q^{k-1}(2q-1)&<(i+1)q^{k-j}-1+q^{k+1}\\ 1&<(i+1)q^{k-j}+q^{k+1}-q^{k-1}(2q-1)\ ,\\ &=q^{k-1}\left((i+1)q^{1-j}+(q-1)^2\right)\end{aligned}$$

and the right inequality holds since it is equivalent to

$$\begin{aligned}q^k(q-1)&>(i+q)q^{k-j}-1\\ q^k\left(q-1-(i+1)q^{-j}\right)+1&\geq q^k\left(q-1-\tfrac{q}{q^j}\right)+1>0.\end{aligned}$$

Case 2-2. Next, the cases where $j = 1$ and $i = 1, \ldots, q-2$ can be shown with the same technique as in Case 2-1: we have

$$T^2\left(\frac{(i+1)q^{k-1}-1}{q^k(2q-1)}\right) = \frac{(i+1)q^{k-1}-1+2q^k}{q^k(2q-1)} \equiv \frac{(i+1)q^{k-1}-1+q^k}{q^k(2q-1)},$$

and $\frac{1}{q} < T\left(\frac{(i+1)q^{k-1}-1}{q^k(2q-1)}\right) < 1$. The left inequality holds since

$$\begin{aligned} q^{k-1}(2q-1) &< (i+1)q^{k-1}-1+q^{k+1} \\ 1 &< q^{k-1}\left(i+2+2q+q^2\right). \end{aligned}$$

However, the right inequality holds only for $i = 1, \ldots, q-2$:

$$\begin{aligned} (i+1)q^{k-1}-1+q^{k+1} &< 2q^{k+1}-q^k \\ -1 &< q^{k+1}-(i+2)q^k = q^k\left(q-(i+2)\right). \end{aligned}$$

Case 3. Lastly, we deal with $j = 1$ and $i = q-1$.

After $2q-1$-iterates, $\frac{q^k-1}{q^k(2q-1)}$ is mapped to itself. We need to show that for any $m < 2q-1$, $T^m\left(\frac{q^k-1}{q^k(2q-1)}\right)$ falls between $\frac{1}{q}$ and 1, hence does not hit any other point in S_2.

If $m = 2l$, $(l = 1, \ldots, q-1)$, then

$$T^m\left(\frac{q^k-1}{q^k(2q-1)}\right) = \frac{q^k-1+2lq^k}{q^k(2q-1)} \equiv \frac{(l+1)q^k-1}{q^k(2q-1)}.$$

We show that

$$\frac{1}{q} < \frac{(l+1)q^k-1}{q^k(2q-1)} < 1.$$

The left-hand inequality is equivalent to

$$\begin{aligned} q^{k-1}(2q-1) &< (l+1)q^k-1 \\ 1 &< (l+1)q^k-q^{k-1}(2q-1) = q^{k-1}\left((l+1)q-(2q-1)\right) = \left((l-1)q+1\right), \end{aligned}$$

and the right-hand inequality is equivalent to

$$\begin{aligned} (l+1)q^k-1 &< q^k(2q-1) \\ -1 &< q^k(2q-2-l). \end{aligned}$$

If $m = 2l+1$, $(l = 1, \ldots, q-2)$, then

$$T^m\left(\frac{q^k-1}{q^k(2q-1)}\right) = \frac{q^k-1+(2l+1)q^{k+1}}{q^k(2q-1)} \equiv \frac{(l+1)q^k-1+q^{k+1}}{q^k(2q-1)}.$$

Again, we show that this does not hit any point in S_2. First it is greater than $\frac{1}{q}$ since

$$\begin{aligned} q^{k-1}(2q-1) &< (l+1)q^k-1+q^{k+1} \\ 1 &< q^{k-1}\left((l+1)q+q^2+(1-2q)\right) = q^{k-1}\left(q^2+(l-1)q+1\right), \end{aligned}$$

and less than 1 since

$$\begin{aligned} (l+1)q^k-1+q^{k+1} &< q^k(2q-1) \\ -1 &< q^k\left(2q-1-(l+1)-q\right) = q^k\left(q-(l+2)\right). \end{aligned}$$

Take γ to be ε above bsc_k. We have thus connected the disconnected segments of $f_r(\text{cyl}_k)$ to construct a waist curve of cyl_{k+1}. □

Figure 7 shows the first few cylinders in this cylinder decomposition for $r = \frac{1}{2}$.

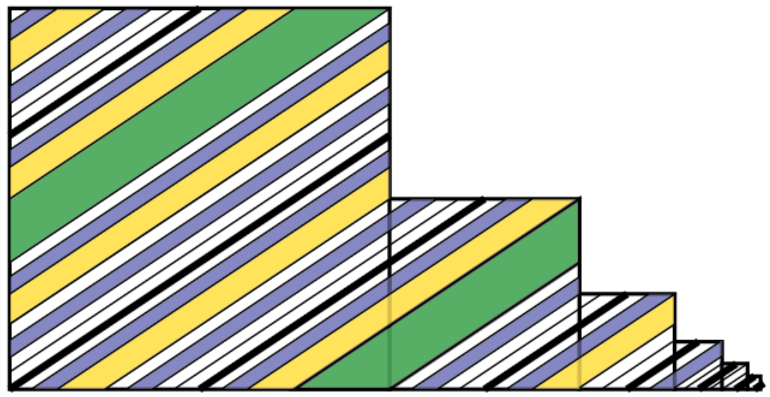

FIGURE 7. Cylinder decomposition on the geometric armadillo tail ($r = 1/2$)

Proposition 4.6. Given a geometric armadillo tail with parameter $r = \frac{1}{q}$, there exists an infinite cylinder decomposition in the $\frac{1}{2-r}$-direction. The number of times cyl_k intersects the y-axis is $2kq - (2k+1)$. Hence the sum of all skew-widths is:

$$\sum_{k=1}^{\infty} (2kq - (2k+1)) \cdot \frac{q-1}{q^k(2q-1)} = \frac{q-1}{2q-1} \sum_{k=1}^{\infty} \left(\frac{2k}{q^{k-1}} - \frac{2k}{q^k} - \frac{1}{q^k} \right)$$
$$= \frac{q-1}{2q-1} \left(\frac{2q^2}{(q-1)^2} - \frac{2q}{(q-1)^2} - \frac{1}{q-1} \right) = 1$$

for all $q \in \mathbb{N} \setminus \{1\}$.

5. AREA OF CYLINDERS

In Lemma 4.4, we found the width of each cylinder. In this section, we will show the length of the waist curve for each cylinder to find the area of cyl_k as a function of q.

First, we will find the horizontal displacement of each waist curve. The table below lists the side lengths of each square and the number of times a waist curve of cyl_k goes through each square. This follows from the circle rotation defined in the previous section.

	$\square_1$	$\square_2$	$\cdots$	$\square_i$	$\cdots$	$\square_k$	$\square_{k+1}$
side length	1	$1/q$		$1/q^{i-1}$		$1/q^{k-1}$	$1/q^k$
#	$k(2q-2)-1$	$(k-1)(q-1)$		$(k-i+1)(q-1)$		$q-1$	1

Then the horizontal displacement of a waist curve of cyl_k is

$$\begin{aligned} & k(2q-2)-1+\frac{1}{q}(k-1)(q-1)+\frac{1}{q^2}(k-2)(q-1)+\cdots+\frac{1}{q^{k-1}}(q-1)+\frac{1}{q^k} \\ = \; & k(2q-2)-1+\sum_{i=1}^{k-1}\frac{(k-i)(q-1)}{q^i}+\frac{1}{q^k} \\ = \; & k(2q-2)-1+\frac{q-1}{q^k}\sum_{i=1}^{k-1}(k-i)q^{k-i}+\frac{1}{q^k} \\ = \; & k(2q-2)-1+\frac{(k-1)q^{k+1}-kq^k+q}{q^k(q-1)}+\frac{1}{q^k}. \end{aligned}$$

For the last equality, we refer to the remark below.

Remark 5.1. The previous computation follows since:

$$\begin{aligned} \sum_{i=1}^{k-i}(k-i)q^{k-i} &= q+2q^2+3q^3+\cdots+(k-1)q^{k-1} \\ &= q+2q^2+3q^3+\cdots+(k-1)q^{k-1}+\left(q+\cdots+q^{k-1}\right)-\left(q+\cdots+q^{k-1}\right) \\ &= 2q+3q^2+\cdots+kq^{k-1}-\frac{q(q^{k-1}-1)}{q-1} \\ &= \left(q^2+\cdots+q^k\right)'-\frac{q^k-q}{q-1} \\ &= \left(\frac{q^2(q^{k-1}-1)}{q-1}\right)'-\frac{q^k-q}{q-1} \\ &= \frac{(k-1)q^{k+1}-kq^k+q}{(q-1)^2}. \end{aligned}$$

Proposition 5.2. The horizontal displacement of the waist curve of cyl_k is

$$(2q-1)\left(k-\frac{q^k-1}{q^k(q-1)}\right)$$

and the actual length of the waist curve, i.e., the circumference of cyl_k is

$$\left(k-\frac{q^k-1}{q^k(q-1)}\right)\sqrt{(2q-1)^2+q^2}.$$

Furthermore, the modulus of cyl_k is given as

$$\frac{\text{circumference}}{\text{width}}=\frac{q^2+(2q-1)^2}{(q-1)^2}\left(kq^{k+1}-(k+1)q^k+1\right),$$

and the area of cyl_k is given by

$$\text{area}\left(\mathrm{cyl}_k\right)=\left(k-\frac{q^k-1}{q^k(q-1)}\right)\frac{q-1}{q^k}.$$

Next, we verify that given $r=1/q$, the infinite sum of $\text{area}(\mathrm{cyl}_k)$ is equal to $\frac{1}{1-r^2}$, hence there exists an infinite cylinder decomposition in the $\frac{1}{2-r}$-direction.

Proposition 5.3. Given a geometric armadillo tail with parameter $r=\frac{1}{q}$, $q\in\mathbb{N}\setminus\{1\}$, we show that

$$\sum_{k=1}^{\infty}\text{area}\left(\mathrm{cyl}_k\right)=\frac{1}{1-r^2}=\frac{q^2}{q^2-1},$$

where the cylinders lie in the $\frac{1}{2-r}$-direction.

Proof. We write area $(\text{cyl}_k) = \frac{k(q-1)}{q^k} - \frac{1}{q^k} + \frac{1}{q^{2k}}$. Following the same spirit as a previous remark, we use $\sum_{i=1}^{\infty} ir^i = \frac{r}{(1-r)^2}$, for $|r| < 1$. The sum of the first terms is

$$\sum_{k=1}^{\infty} \frac{k(q-1)}{q^k} = \frac{q}{q-1}.$$

The second and third terms are geometric sequences, hence we have

$$\sum_{k=1}^{\infty} \text{area}\,(\text{cyl}_k) = \frac{q}{q-1} + \frac{1}{q-1} + \frac{1}{q^2-1} = \frac{q^2}{q^2-1},$$

our desired result. □

6. No parabolic element

Consider the horizontal cylinder decomposition of the armadillo tail seen in Figure 2. The *orthogonal cylinder decomposition* is comprised of exactly the squares. The element $\begin{bmatrix} 1 & 0 \\ 1 & 1 \end{bmatrix}$ is in the Veech group of the surface and this parabolic element corresponds to the perpendicular cylinder decomposition: indeed, the affine map associated with this Veech group element twists these cylinders, but preserves them as a set.

This phenomenon is understood in the finite translation surface setting, where the existence of a cylinder decomposition with rationally related moduli implies a parabolic element in the Veech group and vice-versa. Here, we see that in the perpendicular cylinder decomposition, the modulus of each cylinder is 1 since each cylinder is a square. However, the moduli of the cylinders in the horizontal cylinder decomposition in Figure 2 goes to infinity, and there is no parabolic element in that direction.

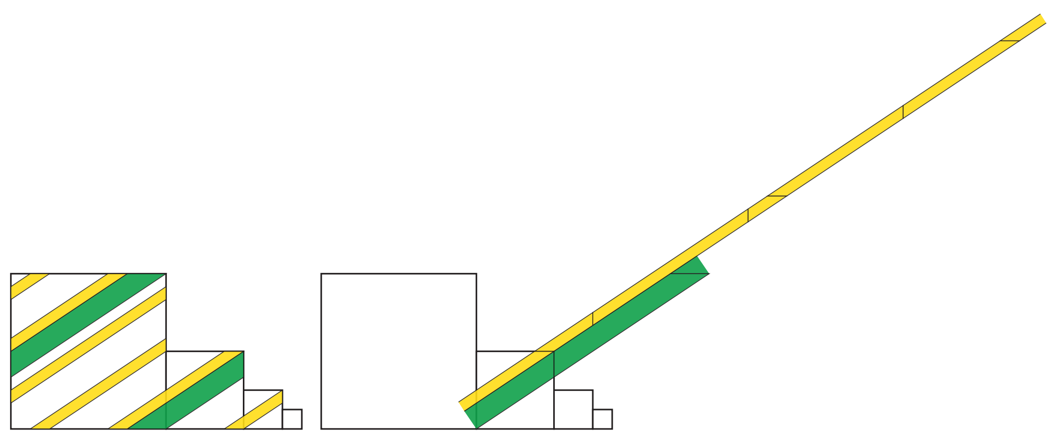

FIGURE 8. Cylinder decomposition $\mathcal{C}$ in the $\frac{1}{2-r}$ direction

Lemma 6.1. Let $\mathcal{C}$ be a cylinder decomposition on a finite area infinite translation surface. Then if the moduli of the cylinders tend to ∞, there is no parabolic element in the Veech group corresponding to an affine map that preserves the cylinder decomposition.

Remark 6.2. The lemma allows for rationally related moduli, hence distinguishes the finite translation surface setting from the infinite translation surface setting.

Proof. Assume otherwise. Then $D\phi$ is a parabolic element in $SL_2(\mathbb{R})$, where the eigendirection corresponds to the direction of the cylinder decomposition. Up to conjugation, $D\phi$ is of the form $\begin{bmatrix} 1 & p \\ 0 & 1 \end{bmatrix}$ for some p. However, there exists a cylinder in the decomposition with circumference greater than p, for any fixed p. This leads to a contradiction since the cylinder cannot be stabilized by $D\phi$. □

Corollary 6.3. Let $\mathcal{C}$ be the cylinder decomposition constructed in the previous sections of this paper. There is no parabolic element in the Veech group corresponding to this cylinder decomposition.

Proof. We observe that the modulus of cyl_k goes to ∞ as k goes to infinity. □

Remark 6.4. In work of Hooper and Treviño [7], they observe that the golden ladder has a cylinder decomposition whose moduli are all equal, and the corresponding perpendicular cylinders are symmetric. They are able to find two parabolics, one in each direction. The construction of these parabolics was described by Thurston in the finite genus case. For the infinite genus case, see [7] or the Hooper–Thurston–Veech construction in [4].

Lemma 6.5. Let $\mathcal{C}$ be the cylinder decomposition constructed in the previous sections of this paper. There is no perpindicular cylinder decomposition.

Proof. □

REFERENCES

[1] Joshua P. Bowman, *The complete family of arnoux–yoccoz surfaces*, Geometriae Dedicata **164** (2012), 113–130.
[2] ———, *Finiteness conditions on translation surfaces* (Yunping Jiang and Sudeb Mitra, eds.), American Mathematical Society, 2012.
[3] Mirko Degli Esposti, Gianluigi Del Magno, and Marco Lenci, *Escape orbits and ergodicity in infinite step billiards*, Nonlinearity **13** (199907).
[4] Vincent Delecroix, Pascal Hubert, and Ferrán Valdez, *Infinite translation surfaces in the wild*, 2024.
[5] W. Patrick Hooper, *The invariant measures of some infinite interval exchange maps*, Geometry & Topology **19** (2015), no. 4, 1895–2038.
[6] W. Patrick Hooper, Pascal Hubert, and Barak Weiss, *Dynamics on the infinite staircase*, Discrete and Continuous Dynamical Systems **33** (2013), no. 9, 4341–4347.
[7] W. Patrick Hooper and Rodrigo Treviño, *Indiscriminate covers of infinite translation surfaces are innocent, not devious*, Ergodic Theory and Dynamical Systems **39** (2015), 2071–2127.
[8] Anja Randecker, *Geometry and topology of wild translation surfaces*, KIT Scientific Publishing, 2016.
[9] Rodrigo Treviño, *On the ergodicity of flat surfaces of finite area*, Geometric and Functional Analysis **24** (2014), 360–386.
[10] Marcelo Viana, *Ergodic theory of interval exchange maps.*, Revista Matemática Complutense **19** (2006), no. 1, 7–100 (eng).

DEPARTMENT OF MATHEMATICS, OKLAHOMA STATE UNIVERSITY, STILLWATER, OK 74075
Email address: dami.lee@okstate.edu

DEPARTMENT OF MATHEMATICS, INDIANA UNIVERSITY, BLOOMINGTON, IN 47405
Email address: jwsouthe@iu.edu